Slope Stabilizing Piles and Pile-Groups: Parametric Study and Design Insights

R. Kourkoulis[1]; F. Gelagoti[2]; I. Anastasopoulos[3]; and G. Gazetas, M.ASCE[4]

Abstract: This paper uses a hybrid method for analysis and design of slope stabilizing piles that was developed in a preceding paper by the writers. The aim of this paper is to derive insights about the factors influencing the response of piles and pile-groups. Axis-to-axis pile spacing (S), thickness of stable soil mass (H_u), depth (L_e) of pile embedment, pile diameter (D), and pile group configuration are the parameters addressed in the study. It is shown that $S = 4D$ is the most cost-effective pile spacing, because it is the largest spacing that can still generate soil arching between the piles. Soil inhomogeneity (in terms of shear stiffness) was found to be unimportant, because the response is primarily affected by the strength of the unstable soil layer. For relatively small pile embedments, pile response is dominated by rigid-body rotation without substantial flexural distortion: the short pile mode of failure. In these cases, the structural capacity of the pile cannot be exploited, and the design will not be economical. The critical embedment depth to achieve fixity conditions at the base of the pile is found to range from $0.7H_u$ to $1.5H_u$, depending on the relative strength of the unstable ground compared to that of the stable ground (i.e., the soil below the sliding plane). An example of dimensionless design charts is presented for piles embedded in rock. Results are presented for two characteristic slenderness ratios and several pile spacings. Single piles are concluded to be generally inadequate for stabilizing deep landslides, although capped pile-groups invoking framing action may offer an efficient solution. **DOI: 10.1061/(ASCE)GT.1943-5606.0000479.**

CE Database subject headings: Slope stability; Embedment; Pile groups; Parameters.

Author keywords: Slope stabilizing piles; Embedment depth; Simplified method; Dimensionless charts; Arching; Pile groups.

Introduction

The use of piles to stabilize slopes is a widely accepted and successfully applied method (Heyman and Boersma 1961; Kitazima and Kishi 1967; Leussink and Wenz 1969; Nicu et al. 1971; De Beer and Walleys 1972; Ito and Matsui 1975; D'Appolonia et al. 1967). Existing design methods can be categorized into pressure or displacement-based (De Beer et al. 1972; Ito and Matsui 1975; Poulos 1995) and numerical methods (Oakland and Chameau 1984; Poulos and Chen 1997). In the first case, the pile is subjected to a presumed slope displacement. This, along with the distribution with depth of the soil modulus and the limiting values of pile-soil contact pressure, have to be prespecified. In the second case (i.e., numerical methods), the problem is analyzed by employing finite elements or finite differences. These methods can presently tackle the entire three-dimensional (3D) problem, taking account of the exact geometry, soil-structure interaction, and pile group effects. Although such methods are in principle the most rigorous, the 3D application is computationally intensive and time-consuming.

[1]Postdoctoral Researcher, National Technical Univ. of Athens, Greece.
[2]Doctoral Candidate, National Technical Univ. of Athens, Greece.
[3]Adjunct Lecturer, National Technical Univ. of Athens, Greece; presently, Research Fellow, Univ. of Dundee, UK.
[4]Professor, National Technical Univ. of Athens, Greece (corresponding author). E-mail: gazetas@ath.forthnet.gr

Note. This manuscript was submitted on December 30, 2009; approved on November 1, 2010; published online on November 4, 2010. Discussion period open until December 1, 2011; separate discussions must be submitted for individual papers. This paper is part of the ***Journal of Geotechnical and Geoenvironmental Engineering***, Vol. 137, No. 7, July 1, 2011. ©ASCE, ISSN 1090-0241/2011/7-663–677/$25.00.

A hybrid methodology for the design of slope-stabilizing piles was presented and thoroughly validated in Kourkoulis et al. (2010). On the basis of the decoupled approach (Viggiani 1981; Hull 1993; Poulos 1995, 1999), combining the simplicity of widely accepted analytical techniques with the advantages of 3D finite-element (FE) modeling, the proposed method involves two steps.

Step 1: Perform conventional slope stability analysis [e.g., using the methods of Bishop (1955), Janbu (1957), Spencer (1967), or Sarma (1973)] to compute the required lateral resisting force (RF) needed to increase the safety factor of the slope to the desired value.

Step 2: Select a pile configuration capable of offering the required RF (to increase the safety factor of the slope to the desired level) for a prescribed deformation level.

A novel approach was developed for the second step, decoupling slope geometry from the computation of pile lateral capacity, thus allowing numerical simulation of a limited region of soil around the piles. The present paper parametrically uses this decoupled analysis method to derive insights about the factors affecting the response of piles and pile-groups. Dimensionless design charts are produced for a specific example to illustrate the effectiveness of the proposed method in practice.

Decoupled Methodology for Pile Lateral Capacity

As schematically illustrated in Fig. 1, Step 2 focuses on a representative region of soil around the pile instead of modeling the whole slope-soil-pile system. The ultimate resistance is computed by imposing a uniform displacement profile onto the boundary of the model, which is a reasonable simplification [as demonstrated by Poulos (1999) and Kourkoulis et al. (2010)]. Having eliminated the detailed slope geometry, a sliding interface at depth H_u is prespecified in the FE model; the piles, of diameter

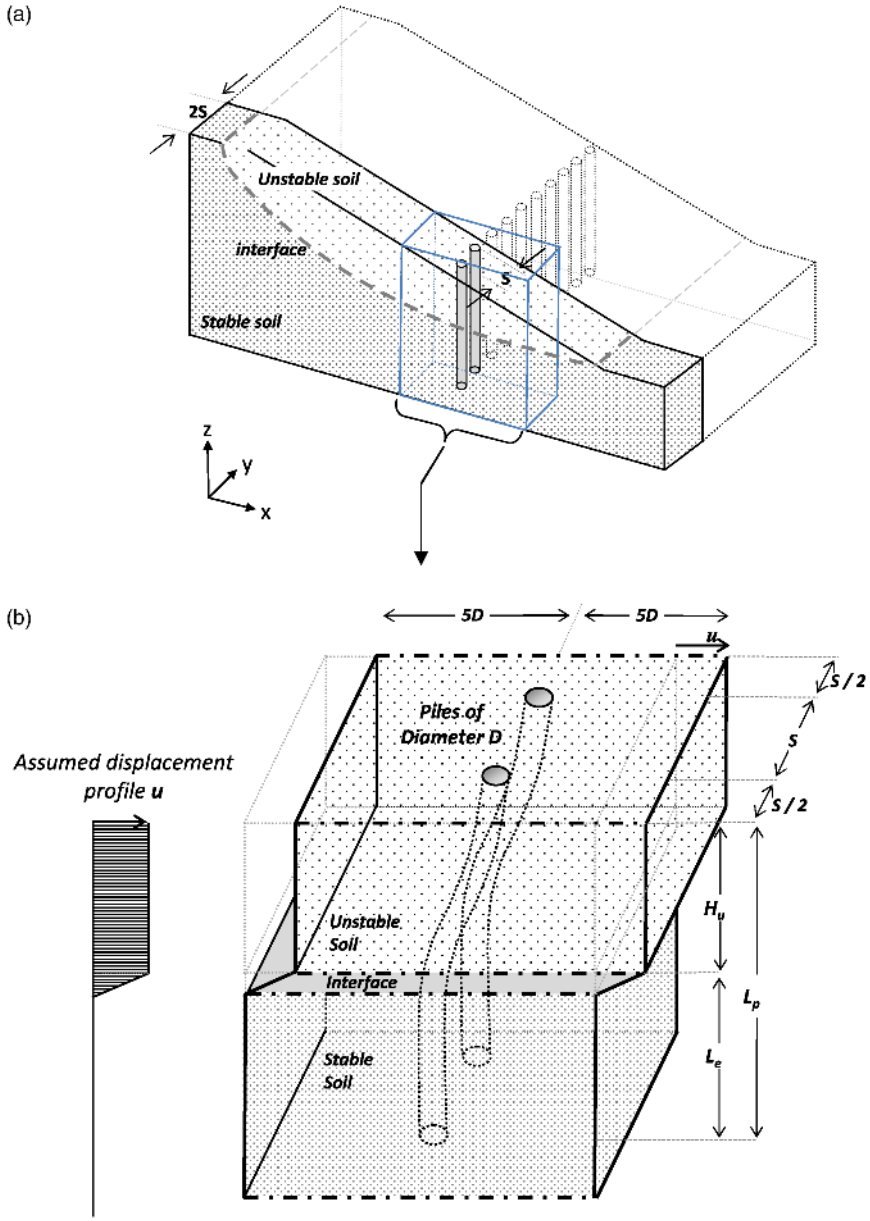

Fig. 1. Schematic illustration of the simplified decoupled methodology for estimation of pile ultimate resistance: (a) instead of modeling the whole slope-soil-pile system, the focus is on the piles and a representative region of soil at its immediate vicinity (blue box); (b) geometry and key parameters of the simplified model

D and length L_p at spacing S, are embedded in the stable soil layer for a length L_e. Given that the zone of influence of each pile does not exceed $5D$ (Reese and Van Impe 2001), the length of the model is restricted to $10D$. The width is equal to $2S$, referring to a representative slice of the slope.

An elastoplastic constitutive model with Mohr-Coulomb failure criterion is used for the soil. The pile is modeled with 3D beam elements, circumscribed by eight-noded hexahedral continuum elements of nearly zero stiffness. As discussed in detail in Kourkoulis et al. (2010), the nodes of the beam are rigidly connected with the circumferential solid element nodes at the same height, so that each pile section behaves as a rigid disk. Analyses are conducted assuming linear or nonlinear pile responses, defined through appropriate moment-curvature (M-c) relations.

Before proceeding to the results of the parametric analysis, the following section briefly discusses the role of soil arching.

Soil Arching between the Piles

Wang and Yen (1974) analytically studied the behavior of piles in a rigid-plastic infinite soil slope with emphasis on arching effects. They concluded that there is a critical pile spacing in both sandy and clayey slopes beyond which almost no arching develops. In general, arching stems from the stress transfer from soil to piles through the mobilization of shear strength. Stress is transferred from yielding parts of a soil mass to adjoining nonyielding or less compliant parts.

A parametric analysis was performed to determine the maximum pile spacing that can still generate sufficient soil arching. The latter is estimated on the basis of the ratio u_{ip}/u_p of interpile ground displacement u_{ip} (i.e., in the middle, between the piles) to the displacement of the piled head u_p after application of the slope displacement. If this ratio is maintained between 1 and 2 (at most),

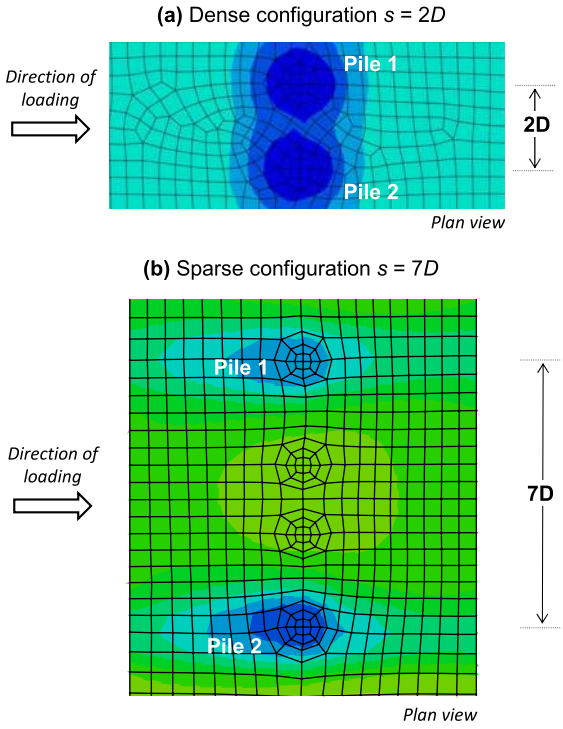

Fig. 2. Soil arching between piles; contours of horizontal displacement (the mesh geometry has been prepared so that two more piles could be modeled in the central part; for the case presented here, these elements have been assigned soil properties): (a) dense pile configuration ($s = 2D$); (b) sparse pile configuration ($s = 7D$)

the pile and the inter-pile soil displace by nearly the same amount and the piles can be considered to be effective in terms of arching. For higher u_{ip}/u_p ratios, the arching effect diminishes. Numerical results were validated by the findings of Prakash (1962), Cox et al. (1984), Reese et al. (1992), and Liang and Zeng (2002), according to which pile spacing $S \leq 5D$ is required to generate a group effect and the associated soil arching between the piles. For $S > 5D$, the piles behave almost as single isolated piles, and the soil will flow between them. Hence, such an arrangement cannot be applied for slope stabilization and will not be further examined. As explained in more detail in the following, $S = 4D$ can be thought of as the most cost-effective arrangement, because it has the largest spacing (i.e., the minimum population of piles) required to produce soil arching between the piles for the inter-pile soil to be adequately retained. This is consistent with both common engineering practice (the $s = 4D$ spacing is utilized as the optimal pile spacing in slope stabilization applications) and numerous research findings (Smethurst and Powrie 2007; Pradel and Carrillo 2008].

Fig. 2 provides an illustrative comparison between two extreme cases: a very dense configuration in which pile spacing is $S = 2D$, where soil arching is guaranteed, and a sparse configuration with large spacing $S = 7D$, where the piles are so distant that soil flows between them (i.e., no arching develops). The unstable soil layer is considered to be a loose silty sand: $\varphi = 28^\circ$, $\psi = 2^\circ$, and $c = 3$ kPa. The stable (bottom) layer is very hard soil, bordering on soft rock, of $S_u = 600$ kPa. The interface, representing the sliding plane of the slope, is located at depth $H_u = 4$ m; its properties are: $\varphi = 16^\circ$, $\psi = 1^\circ$, and $c = 3$ kPa. Fig. 2(a) plots the displacement contours on the ground surface for $D = 1.2$ m and $S = 2D$. The distribution of displacement contours shows that the interpile soil displaces almost the same amount with the piles (i.e., $u_{ip} \approx u_p$), which is a very clear manifestation of strong arching. In stark contrast, for $S = 7D$, the inter-pile soil is hardly confined by the piles and flows between them: u_{ip} is substantially larger than u_p [Fig. 2(b)].

Parametric Analysis

The following discusses the results of a detailed parametric analysis of the problem. Both cohesive and noncohesive soils have been utilized to model the unstable layer. The interface depth H_u from the surface is also varied parametrically, from 4–12 m: shallow and (relatively) deep slide, respectively. The following key response factors are examined:

1. The effect of pile nonlinearity;
2. The effect of pile spacing;
3. The inhomogeneity of the unstable soil layer;
4. The strength of the stable soil layer; and
5. The depth of pile embedment into the stable layer.

Effect of Pile Structural Nonlinearity

An example is presented for the same soil and pile configuration, referring to the nonlinearity of the reinforced concrete pile. This is introduced in the FE analysis through appropriate cross-sectional moment-curvature relations, computed for a steel reinforcement ratio of 4%. This choice was based on an initial sensitivity analysis, which revealed that the most cost-effective solution is to install the least amount of piles with the maximum practically attainable reinforcement. Although allowable by codes, this amount of reinforcement will undoubtedly result in quite a dense reinforcement cage, so in practical applications, a 2–3% reinforcement ratio is usually the limit. Because the pile moment capacity depends on its diameter and reinforcement ratio, a decrease of the reinforcement will require an increase of pile diameter for its moment capacity to remain the same. Table 1 summarizes the effect of reinforcement ratio on pile moment capacity for some typical pile dimensions, as calculated through reinforced concrete (C30, S500) section analysis using *XTRACT* software. The results in Table 1 show that for the typical cases examined, a pile of diameter D and reinforcement ratio of 4% yields approximately the same moment capacity with a pile with of 3% reinforcement ratio and diameter $1.1D$, or with a pile of diameter $1.2D$ (= 1.2 m) and 2% reinforcement ratio. Hence, the results presented in the following

Table 1. Ultimate Pile Structural Moment Capacity for Different Pile Diameters and Reinforcement Ratios

Pile diameter (m)	Reinforcement ratio	M_{ult} (MN)
1	0.04	4.5
	0.03	3.5
	0.02	2.7
1.1	0.04	6
	0.03	4.5
	0.02	3.5
1.2	0.04	7.5
	0.03	6
	0.02	4
1.4	0.04	13
	0.03	10
	0.02	7

Note: concrete strength C30, steel strength S500.

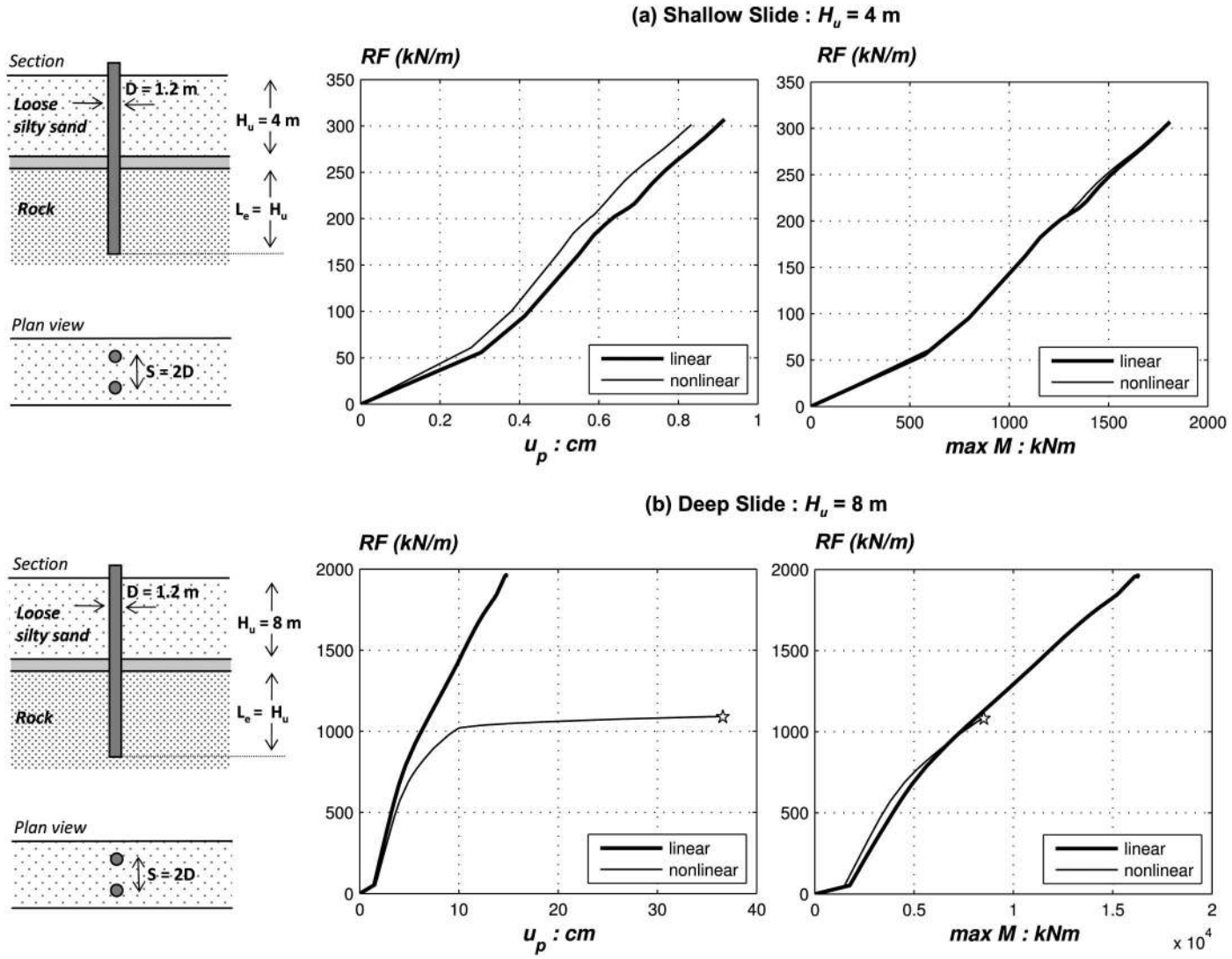

Fig. 3. The effect of pile nonlinearity; pile RF with respect to pile head displacement u_p and maximum bending moment M for elastic and nonlinear piles: (a) shallow slide, $H_u = 4$ m; and (b) relatively deep slide, $H_u = 8$ m

(which refer to 4% reinforcement ratio), may be generalized for lower reinforcement ratios.

Fig. 3 compares the response of an elastic pile to that of a nonlinear pile, both subjected to lateral soil displacement for two slide scenarios: a shallow ($H_u = 4$ m) and a relatively deep ($H_u = 8$ m) slide. In the shallow slide [Fig. 3(a)], soil failure dominates the behavior of the system; the depth $H_u = 4$ m is not enough to drive the pile to its ultimate structural capacity. Hence, pile nonlinearity does not make a difference. In marked contrast, for the deep slide ($H_u = 8$ m), the differences are quite pronounced [Fig. 3(b)]. Now, the moving soil is deep enough to impose a large enough thrust for the pile to reach its ultimate structural capacity. However, as long as the pile has not reached its yielding curvature, the response is not affected by pile inelasticity. Hence, these parametric analyses assume elastic pile response; the results are roughly applicable to nonlinear piles, as long as they do not reach their ultimate curvature.

Effect of Pile Spacing

Fig. 4 illustrates the effect of pile spacing for various slide depths: a shallow ($H_u = 4$ m) and a deep ($H_u = 8$ m) slide, and an intermediate case ($H_u = 6$ m). The results refer to the preceding pile and soil configuration ($D = 1.2$ m piles in idealized loose silty sand). The pile embedment length is equal to the unstable soil thickness H_u (corresponding to full fixity conditions of the pile in the stable ground). The following trends are noteworthy:

1. The smaller the spacing of the piles, the greater is the force offered per unit width. Although the decrease of pile spacing increases the resistance force per unit width, their effectiveness (i.e., the resistance force per pile) is decreased owing to pile-to-pile interaction (i.e., the group effect).
2. As the spacing increases, the pile displacement u_p necessary to yield a specific RF increases. Although it may be misleadingly concluded that approximately the same ultimate force can be offered by all configurations examined (developed at a different level of displacement in each case), this is valid for elastic piles only. If the ultimate structural capacity of the pile is taken into account, the ultimate RF depends largely on pile spacing, even if there were no restrictions in terms of allowable displacement. To further elucidate this point, the dotted line in Fig. 4(b) shows the ultimate bending moment capacity M_{ult} of the $D = 1.2$ m pile, which is approximately 7.2 MNm (with the maximum possible reinforcement of 4%). Its intersection with the RF curves corresponds to the ultimate realistic RF_r that can be offered by the respective pile configuration. Evidently, RF_r (in terms of resistance per unit width) increases

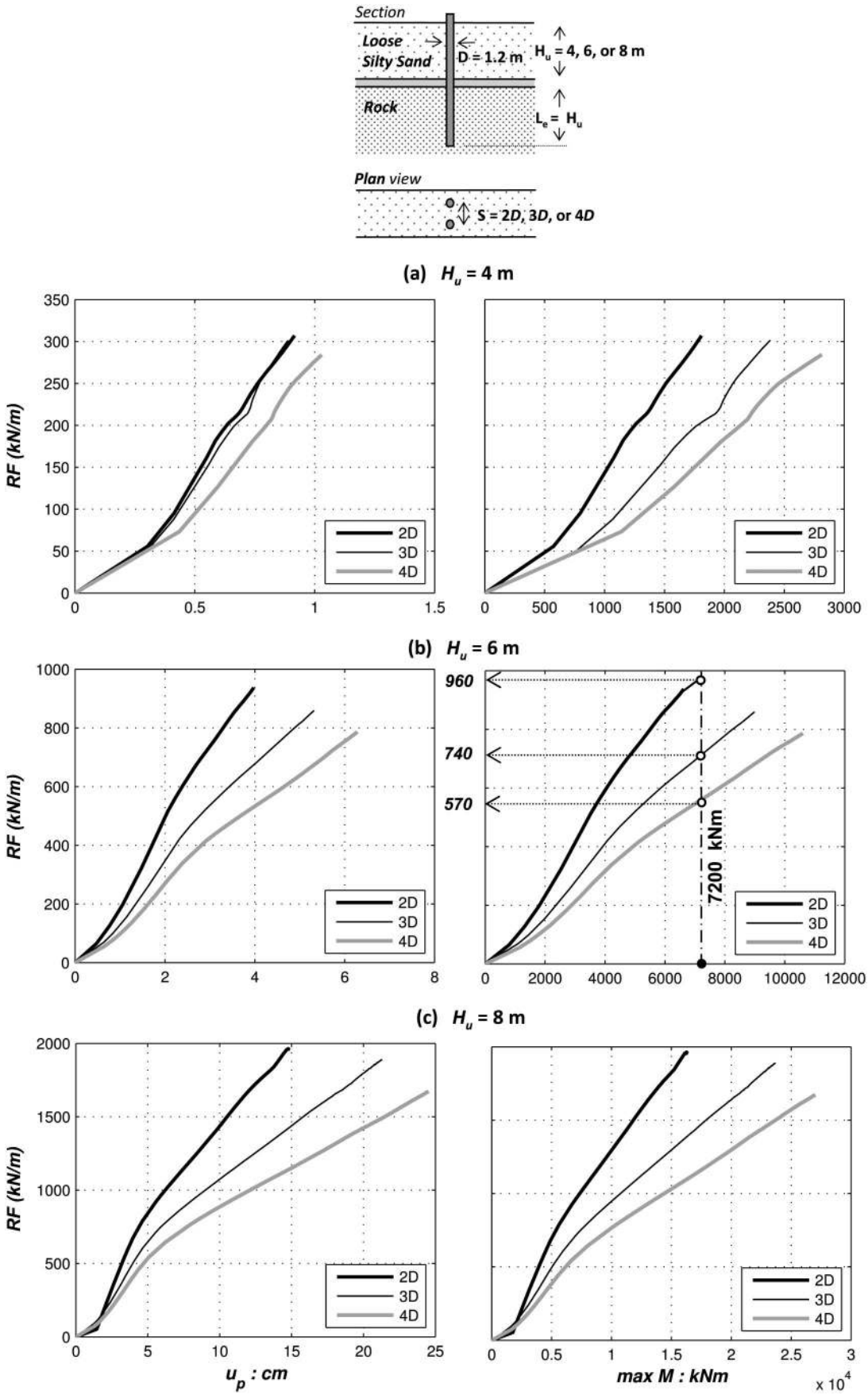

Fig. 4. The effect of pile spacing; RF offered by the pile with respect to pile head displacement u_p and maximum bending moment M, for: (a) a shallow landslide of $H_u = 4$ m; (b) an intermediate landslide of $H_u = 6$ m; (c) a relatively deep landslide of $H_u = 8$ m

with the decrease of pile spacing S: $RF_r \approx 960$, 740, and 570 kN/m, for $S = 2D$, $3D$, and $4D$, respectively. In contrast, if RF_r per pile is considered, the conclusion will be the opposite: $RF_r \approx 2300$ kN for $S = 2D$ ($= 960$ kN/m $\times$ 2.4 m); 2660 kN for $S = 3D$; and 2740 kN for $S = 4D$. This is why $S = 4D$ is usually the most cost-effective solution. The pile deflection u_p for which RF_r is attained also changes with S.

3. In the case of a shallow $Hu = 4$ m slide [Fig. 4(a)], RF is marginally dependent on pile spacing. Owing to the relatively small depth of the interface, the pile behaves as rigid and the response resembles that of a retaining wall or a caisson. As a result, group effects do not seem to play an important role, and RF is almost independent of S. However, this is not true for the pile bending moment M required to generate the desired RF, which depends substantially on S (see previous discussion).
4. Owing to the increased thickness of the sliding soil mass for a deep $H_u = 8$ m slide [Fig. 4(c)], the pile behaves as flexible and group effects play an increasingly important role. As a result, RF becomes more sensitive to S. Hence, the flexibility of the soil-pile system does not only depend on pile spacing, but is primarily governed by the depth of the sliding soil mass.

Effect of Soil Inhomogeneity

The effect of soil inhomogeneity, in terms of the distribution of the shear modulus G with depth, has been thoroughly investigated by Kourkoulis (2009). Homogeneous soil layers (i.e., of constant G) were compared to nonhomogeneous, assuming a linear increase of G with depth but keeping the same mean value with the homogeneous soil, to facilitate comparisons. For the cases examined, the effect of soil inhomogeneity was found to be of secondary importance. Only in the shallow $H_u = 4$ m slide were the results barely affected. The key conclusion is that the response is primarily affected by the strength of the unstable layer and not by the distribution of stiffness.

Effect of the Strength and Stiffness of the Underlying Stable Ground

The strength and stiffness of the stable ground were investigated parametrically with model materials ranging from relatively loose sand to a rock-type material. The idealized soils of the stable ground layer are as follows:

1. Loose silty sand: $\phi = 28^\circ$, $\psi = 2^\circ$, $c = 3$ kPa, $G = 16$ MPa.
2. Dense sand: $\phi = 38^\circ$, $\psi = 2^\circ$, $c = 3$ kPa, $G = 32$ MPa.
3. Soft rock: $\phi = 45^\circ$, $\psi = 5^\circ$, $c = 50$ kPa, $G = 1.2$ GPa.
4. Rock: $\phi = 45^\circ$, $\psi = 5^\circ$, $c = 100$ kPa, $G = 4$ GPa.

The strength parameters of the stable soil layer were chosen so that the ultimate passive soil pressure provided by the stable soil layer $(P_u)_{\text{stable}}$ is greater or equal to the ultimate passive soil pressure $(P_u)_{\text{unstable}}$ developing in the unstable layer. For cohesionless soil, the latter is given by (Broms 1964):

$$(P_u)_{\text{unstable}} = aK_p\sigma'_{vo} \tag{1}$$

where α = a parameter ranging between 3 and 5; K_p = passive earth pressures coefficient; and σ_{vo} = overburden stress. For cohesive soil of undrained shear strength S_u:

$$(P_u)_{\text{unstable}} = N_p S_u \tag{2}$$

where N_p = a parameter ranging between 9 and 12 (Matlock 1970).

Thus, the strength parameters of the four idealized stable ground soils yield the following ratios of $(P_u)_{\text{stable}}$ to $(P_u)_{\text{unstable}}$ (Kourkoulis 2009):

1. $P_{\text{ustable}} = (P_u)_{\text{unstable}}$ for loose silty sand;
2. $(P_u)_{\text{stable}} = 1.6(P_u)_{\text{unstable}}$ for dense sand;
3. $(P_u)_{\text{stable}} = 3(P_u)_{\text{unstable}}$ for soft rock; and
4. $(P_u)_{\text{stable}} = 6(P_u)_{\text{unstable}}$ for rock.

In all cases examined, the embedment depth L_e of the pile into the stable layer was assumed equal to $2H_u$, so that full fixity conditions could be guaranteed (although for the rock cases such depth is not necessary).

As shown in the example of Fig. 5, the analysis reveals that a pile embedded in a substratum of relatively low strength (dense sand) cannot provide the same level of ultimate RF as when embedded in a stiff substratum (rock), unless it is excessively deformed. However, this increase in displacement [Fig. 5(a)] is not associated with a proportional increase in pile bending moments [Fig. 5(b)]. Because the shear strength of the weaker soil substratum is mobilized along the whole length of the pile, the deflection of the pile is distributed throughout almost its whole length, and thereby does not generate a proportional increase in M [Fig. 5(c)]. In contrast, when the stable ground is stiff, the flexural distortion of the pile is more localized (close to the sliding interface), generating proportionally larger M. In the case of stiff substratum conditions (rock), the point of fixity, where the maximum M takes place, is located at the interface level; for softer, more compliant substratum (dense sand), the point of fixity is shifted deeper into the stable ground. The two deformed mesh snapshots with superimposed lateral displacement contours in Fig. 6 further illustrate this key difference in response.

Effect of Pile Embedment

The strength of the underlying (stable) stratum influences the amount of lateral displacement necessary for the development of the ultimate RF that can be offered by the pile. It is therefore assumed that the embedment depth necessary to achieve the ultimate RF will be a function of the stable soil strength. The critical embedment depth is sought, beyond which the passive resistance offered by the pile remains unaltered for the same level of pile deformation. The following values of total embedment depth L_e are parametrically investigated: $L_e = 0.7H_u$, $1.0H_u$, $1.2H_u$, and $1.5H_u$.

Fig. 7 presents analysis results in terms of RF for $P_{\text{ustable}} = (P_u)_{\text{unstable}}$, which corresponds to a conservative scenario in which the strength of the stable stratum is equal to that of the unstable. Snapshots of deformed mesh with superimposed plastic strain are compared in Fig. 8 for the two extremes: $L_e = 0.7H_u$ and $1.5H_u$. For the small embedment length ($L_e = 0.7H_u$) the pile is rigid and its response resembles that of a caisson [Fig. 8(a)]: rigid-body rotation without substantial flexural distortion. Thus, despite the great displacement at its head which exceeds 50 cm [Fig. 7(a): $u_p > 50$ cm], practically following the movement of soil, the pile does not develop substantial bending moment [Fig. 7(b)].

This finding is consistent with Poulos's (1999) description of the short pile mode of failure, which involves mobilization of the stable soil strength and failure of the soil underneath the pile. Therefore, the pile structural capacity is not adequately exploited, and such a design would not be economical. To utilize the full pile structural capacity, a larger embedment depth is required (as L_e increases, so does the ability of the stable stratum to provide fixity conditions). Pile flexure rather than pile rotation becomes increasingly prevalent for embedment depths exceeding $1.2H_u$, as vividly portrayed in Fig. 8(b). However, if the stable stratum is of high strength, the increase of embedment length will unavoidably be associated with an increased installation cost. Such cost implications have not been examined in this paper.

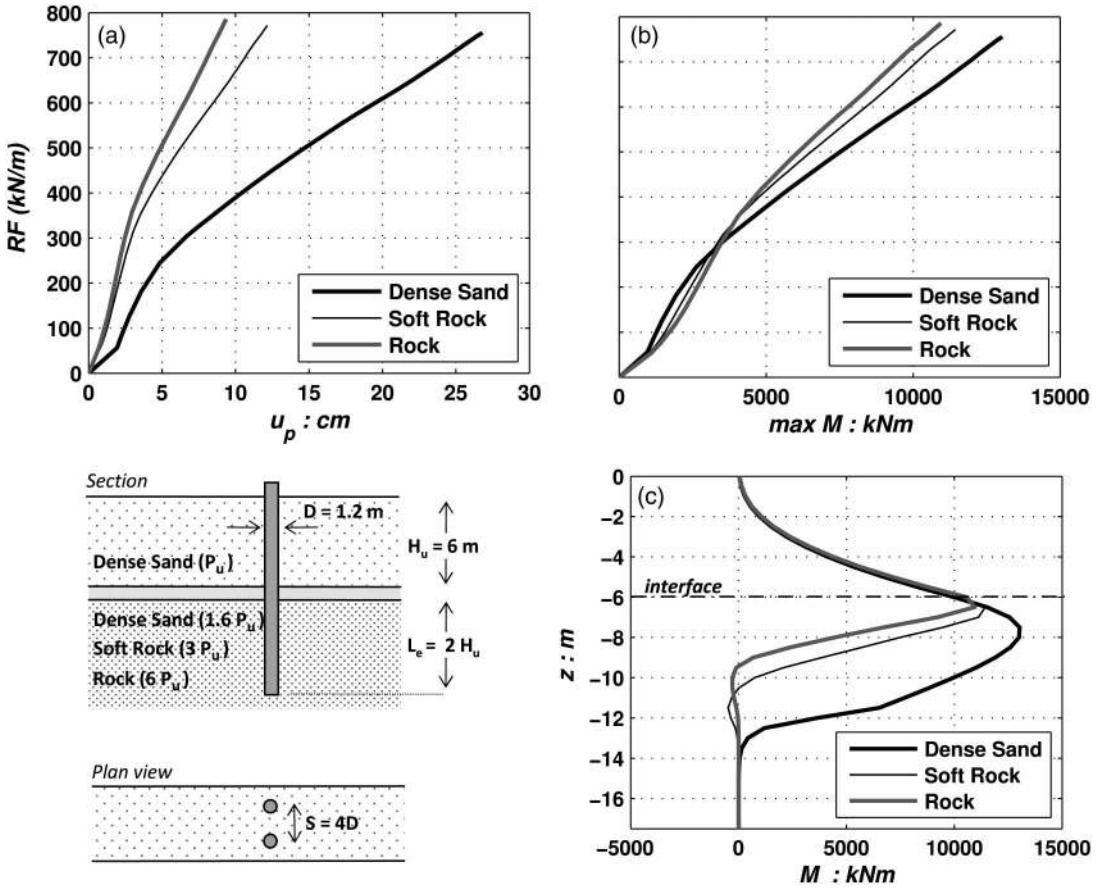

Fig. 5. The effect of the stiffness and strength of the stable ground; comparison of three idealized stable ground soil layers: (a) RF offered by the pile with respect to pile head displacement u_p; (b) RF with respect to the maximum bending moment M; (c) distribution of pile bending moment M with depth

When the stable soil strength becomes larger than that of the unstable soil, $(P_u)_{\text{stable}} = 1.6(P_u)_{\text{unstable}}$, the discrepancies among different embedment depths become less pronounced (Fig. 9). This implies the existence of a critical embedment depth L_e, which is of the order of $1.2H_u$ in this case: the RF curves for $1.2H_u$ and $1.5H_u$ practically coincide. For $L_e = 0.7H_u$, the embedment is not enough to provide adequate fixity conditions. The response for $L_e = 1.0H_u$ tends to approach the behavior of the even deeper embedded piles. This result is consistent with Poulos's suggestion (1999) that the critical or effective length of the pile in the stable soil layer should be at least equal to H_u (for a pile embedded into a stable soil of ultimate resistance $2P_u$, i.e., two times the resistance of the unstable soil). This means that, for economical design, the pile length in the stable layer should not exceed the elastic critical length of the pile in that layer, as calculated by Poulos and Hull (1989), Gazetas and Dobry (1984), and Randolph (1981).

The behavior of piles embedded in an even stronger substratum, $(P_u)_{\text{stable}} = 3.0(P_u)_{\text{unstable}}$, is explored in Fig. 10. The response is now essentially insensitive to L_e: the RF curves for $L_e \geq H_u$ almost coincide. A slight discrepancy can only be observed for $L_e \geq 0.7H_u$ in the plot of RF with respect to the pile head displacement u_p [Fig. 10(a)], which does not cause any increase in the value of the developing bending moment M [Fig. 10(b)]. This implies that the critical embedment length may be even lower than $1.0H_u$, and quite close to $0.7H_u$.

For even stronger stable soil, $(P_u)_{\text{stable}} = 6.0(P_u)_{\text{unstable}}$, for which the results are not shown here, the critical embedment length is even lower than $0.7H_u$.

Dimensional Analysis

In an attempt to produce dimensionless design charts, a dimensional analysis is conducted. This refers to reinforced concrete piles embedded in rock and considers only the flow mode type of failure (Poulos 1999). The embedment length (L_e) is assumed equal to the unstable soil layer depth (H_u), which has been found adequate to provide fixity conditions, as discussed previously.

According to the Vaschy-Buckingham Π-theorem (Langhaar 1951; Barenblatt 1996; Palmer 2008), the terms involved in the calculation of the pile ultimate load may be combined to form three independent dimensionless variables. For the case of cohesionless soil, this study adopts the following correlation among independent variables:

$$\frac{\text{RF}}{3K_pD\gamma H_u^2} = f\left(\frac{u_pH_u^3}{10D^4}, \frac{S}{D}, \frac{H_u}{D}\right) \tag{3}$$

The term $u_pH_u^3/10D^4$ will be referred to as the dimensionless pile displacement, and $\text{RF}/(3K_pD\gamma H_u^2)$ represents the dimensionless resistance force. The term S/D apparently represents the pile spacing normalized to the pile diameter, and H_u/D is the pile slenderness ratio.

The results of this dimensional analysis are depicted in Fig. 11 for piles embedded through loose silty sand (unstable layer) in rock (stable layer), for two slenderness ratios:

1. $H_u/D = 3$, which represents a rigid soil-pile system; and
2. $H_u/D = 5$, for a moderately flexible soil-pile system.

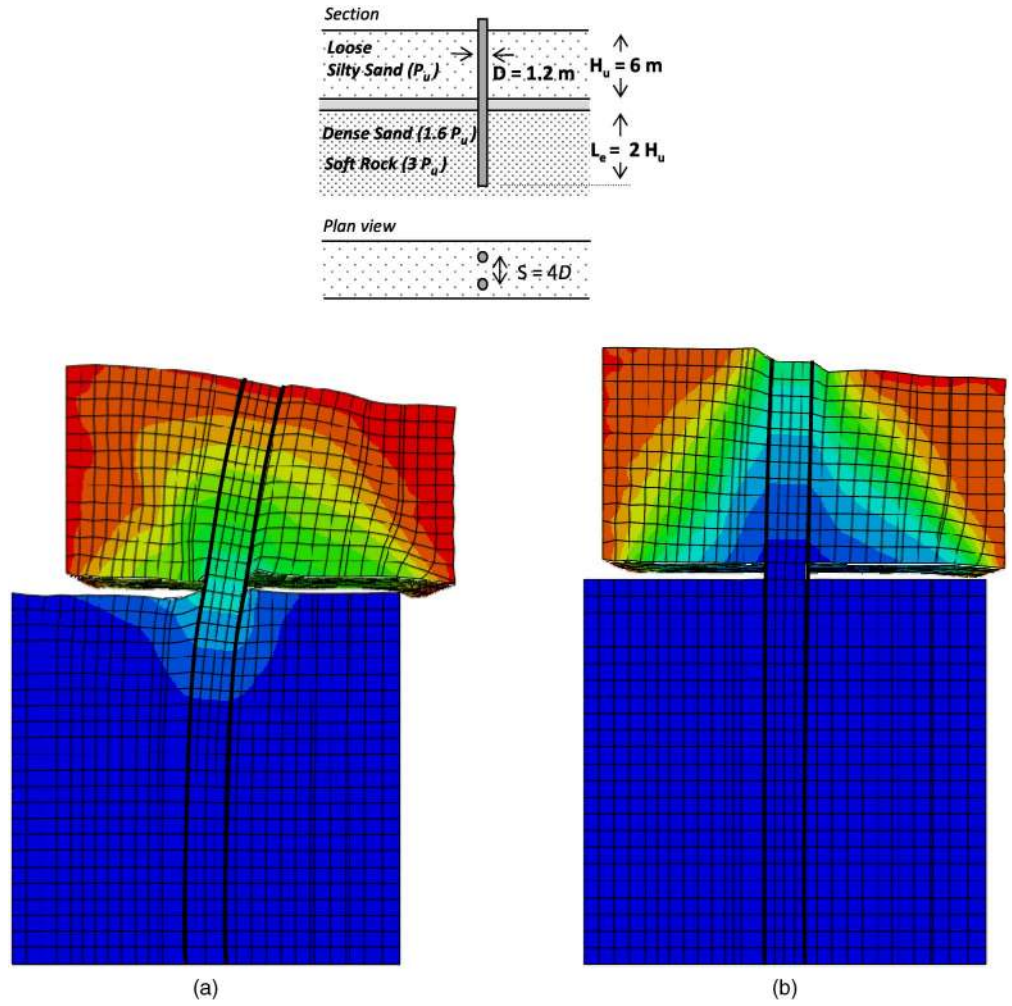

Fig. 6. The effect of the stiffness and strength of the stable ground; snapshots of deformed mesh with superimposed lateral displacement contours for: (a) pile embedded in relatively soft, compliant stable ground soil (dense sand, $1.6p_u$); (b) pile embedded in less compliant soft rock ($3p_u$) (the soil in the failure zone has been omitted from the picture for clarity)

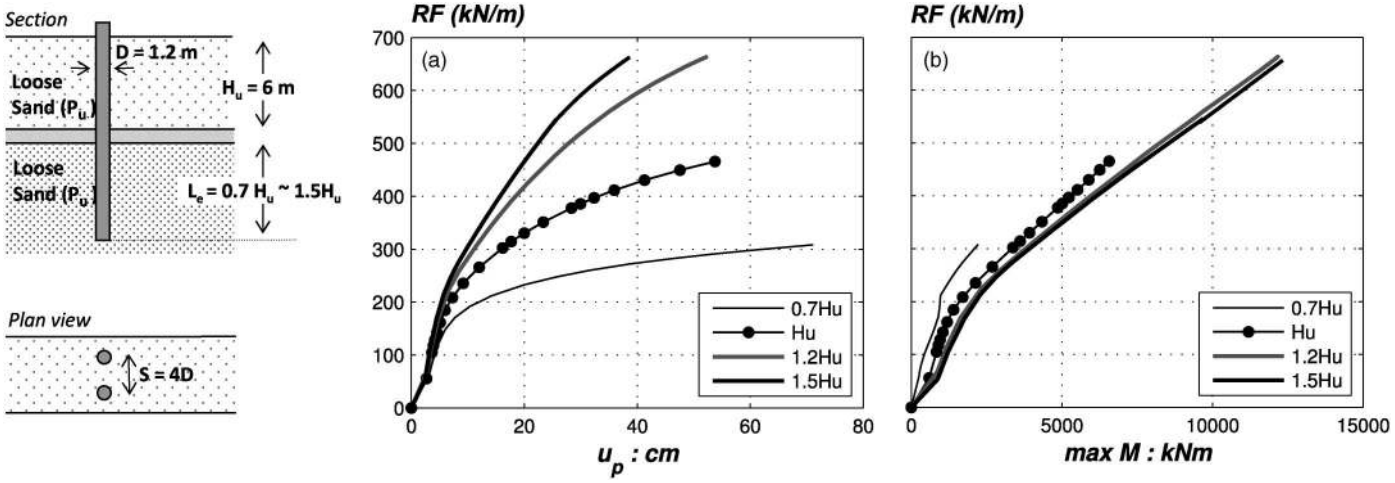

Fig. 7. The effect of pile embedment length on the RF offered by the pile with respect to (a) pile head displacement u_p; (b) maximum bending moment M [strength of stable soil equal to of unstable $(P_u)_{\text{stable}} = (P_u)_{\text{unstable}}$]

For two (extreme) cases of pile spacing :

1. $S/D = 2$, which represents very densely spaced piles; and
2. $S/D = 4$, for piles spaced at the optimum distance (see previous discussion).

For the rigid system, the results follow a very well defined line for both S/D ratios. In contrast, for the flexible system, the results are more scattered, especially for $S/D = 4$ [Fig. 11(b)]. This deviation from a single line is more prominent as the passive

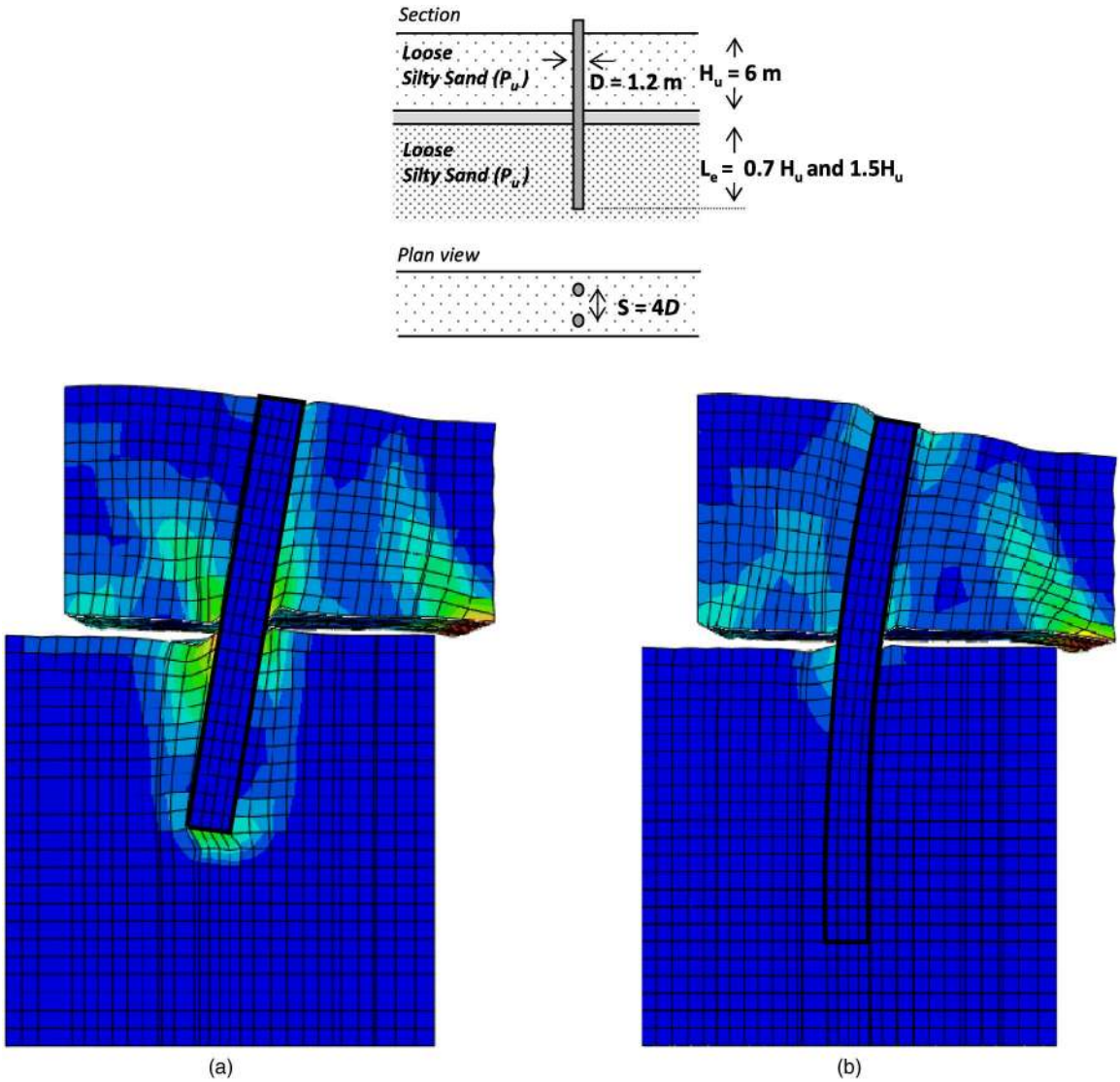

Fig. 8. The effect of pile embedment length; snapshots of deformed mesh with superimposed plastic strain contours for pile embedded into the stable ground: (a) $0.7H_u$; (b) $1.5H_u$

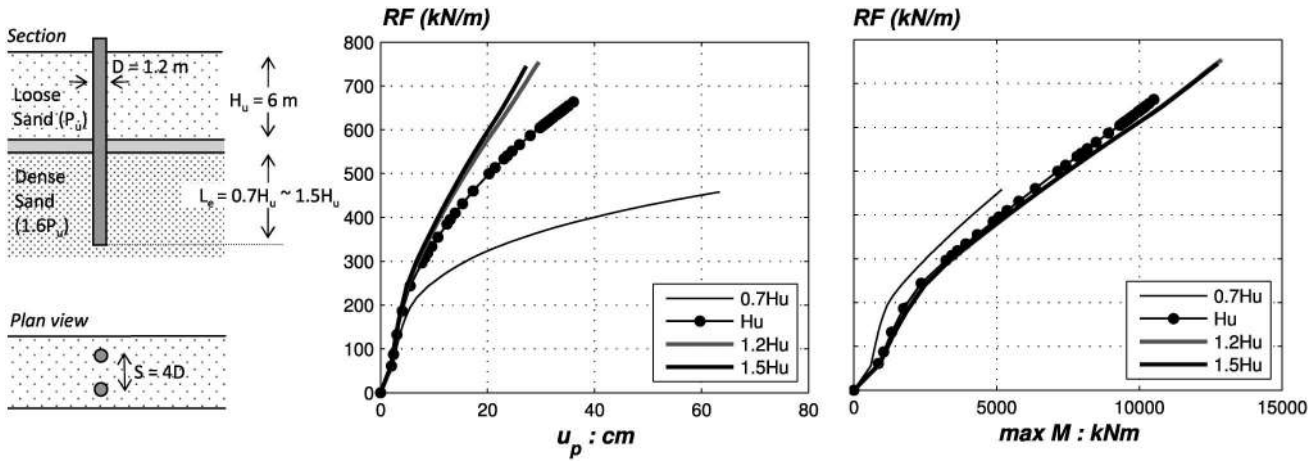

Fig. 9. The effect of pile embedment length on the RF offered by the pile with respect to (a) pile head displacement u_p; (b) maximum bending moment M [strength of stable soil larger than that of unstable $(P_u)_{\text{stable}} = 1.6(P_u)_{\text{unstable}}$]

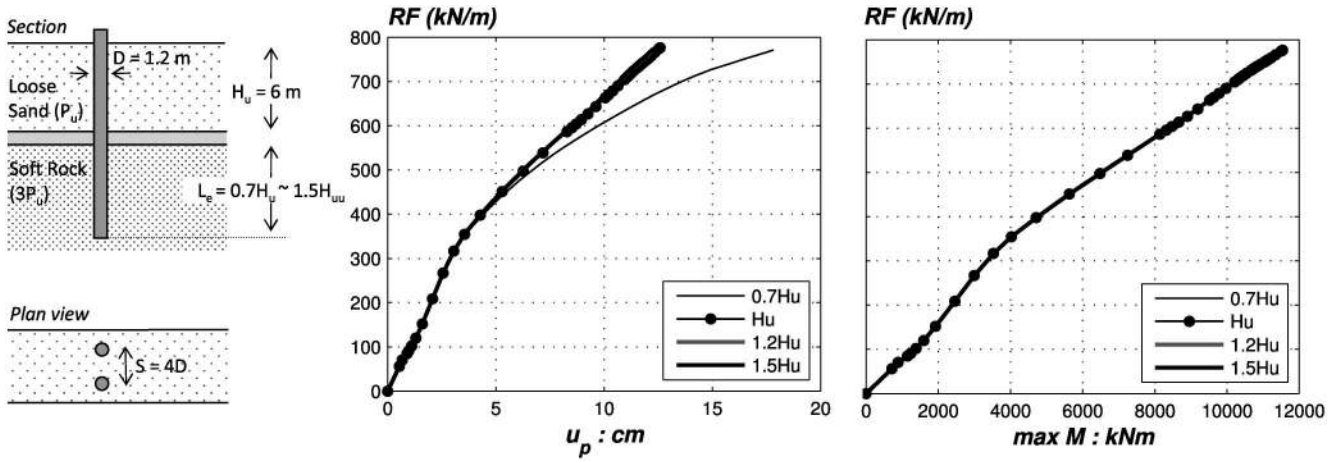

Fig. 10. The effect of pile embedment length on the RF offered by the pile with respect to (a) pile head displacement u_p; (b) maximum bending moment M [strength of stable soil much larger than that of unstable $(P_u)_{\text{stable}} = 3(P_u)_{\text{unstable}}$]

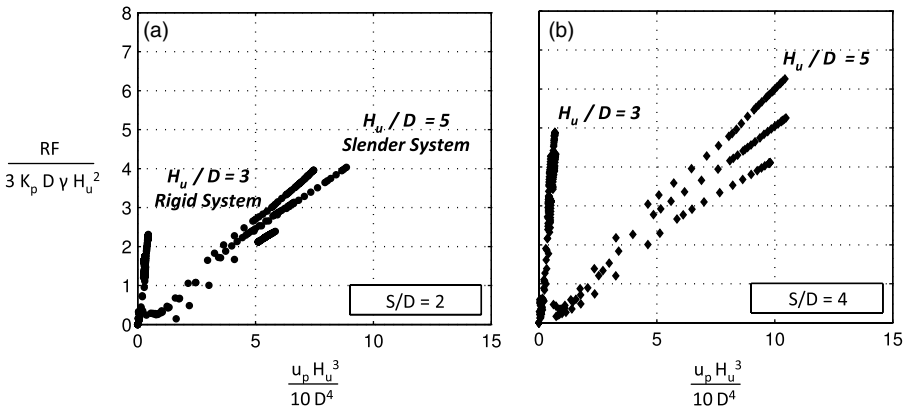

Fig. 11. Dimensional analysis results for piles embedded through loose silty sand (unstable layer) in rock (stable layer); dimensionless pile resistance force with respect to dimensionless pile displacement for rigid $(H_u/D = 3)$ and slender $(H_u/D = 5)$ systems, and pile spacing: (a) $S/D = 2$; (b) $S/D = 4$

resistance term increases. The maximum deviation from the linear prediction is of the order of 15% for $S/D = 2$, reaching almost 25% for $S/D = 4$. This difference is primarily attributed to the estimation of the passive resistance of the soil. Indeed, the expression $P_u = 3K_pD\gamma H_u^2$ is a lower estimate. As suggested by various researchers (Reese and Van Impe 2001; Poulos 1999; Viggiani 1981; Randolph and Houlsby 1984), the pile ultimate passive resistance is actually $P_u = aK_pD\gamma H_u^2$, with α varying between 3 and 5. Hence, the selection of $\alpha = 3$ unavoidably underestimates the pile resistance in some cases. However, for design purposes, the most conservative approach is justified. This effect is more evident when the soil pile system behavior diverges from the wall-type behavior (i.e., when the slenderness or the spacing ratio increases).

These charts may be used to provide a preliminary design of the pile configuration that is able to rise the slope safety factor to the acceptable level. To this end, as shown earlier, the designer of the stabilization of a landslide with depth H_u (in m) must first perform a conventional slope stability analysis (Step 1 of the methodology) to estimate the required RF (in kN) value. Then, using the design charts, the designer can estimate which pile configuration [i.e., pile diameter D (in m) and spacing S (in m)] is capable of producing the required RF at acceptable displacement u_p (in m). To use these nondimensional charts, the designer will first need to decide upon an initial pile diameter and acceptable head displacement u_p to calculate the X value of the chart. Then, initially for the more economical spacing of $S/D = 4$, the designer may calculate the RF value from the charts. If this is insufficient, a further attempt may be made for the denser pile spacing of $S/D = 2$. If an even higher RF value is still required, then the pile diameter should be increased.

Slope Stabilization through Alternative Pile Group Configurations

As revealed by the previously presented analyses, single piles may be inadequate for stabilizing deep landslides. Following the previous dimensional analysis, when the slenderness ratio H_u/D is lower than 3, the response of the system can be characterized as flexible. For significantly smaller slenderness ratios $(H_u/D < 1)$, the system becomes too flexible and the sliding mass cannot be stabilized (Kourkoulis 2009). In such cases, the use of pile group configurations may provide a more reasonable solution.

Mechanism of Load Transfer in Pile-Groups: The Advantage of the Pile Frame

Fig. 12 schematically illustrates the theoretical disparity between single piles and pile-groups in terms of the mechanism of bending moment development. The pile group comprises two parallel rows

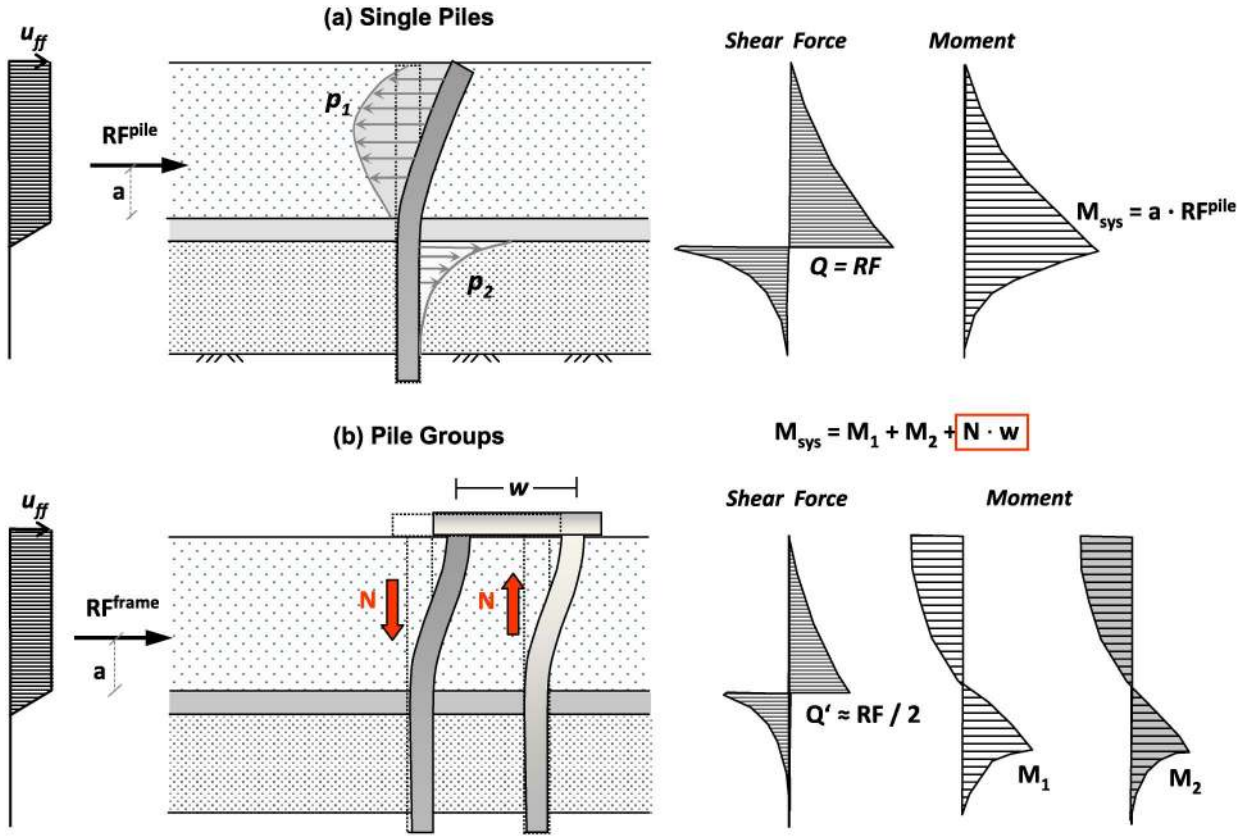

Fig. 12. Comparison of load transfer mechanism for (a) single piles; (b) pile-groups, in which part of the load is converted to axial load, partially relieving the piles from bending distress, owing to frame action

of piles (along the direction of slippage), connected through a rigid pile cap. Apparently, each pair of piles with caps constitutes a frame. The distance between the front and the rear row of piles (frame arm) is defined as w. In the direction normal to slippage, the spacing S of the pile frames is assumed to be equal to that of single piles.

In the case of single piles [Fig. 12(a)], the displacement of the unstable layer toward the resisting pile results in the generation of passive earth pressures in the upper part of the pile. To develop its reaction force, the lower part of the pile within the stable layer tends to displace opposite to the direction of soil movement, again producing passive earth pressures. The pressures acting along the piles result in the development of internal forces, as indicated in Fig. 12(a). The uniform displacement profile u_{ff} imposed at the free field will generate a reaction force $\mathrm{RF}^{\mathrm{pile}}$ at height $a \approx H_u/3$ from the interface level, assuming linear distribution of soil pressures with depth, and the system moment $M_{\mathrm{sys}} = \mathrm{RF}^{\mathrm{pile}} xa$ must be undertaken by a single pile.

In contrast, in the case of the pile group [Fig. 12(b)], the developing frame action leads to the distribution of the total load into two piles through the pile cap. Hence, the total moment distribution can be analyzed as

$$M_{\mathrm{sys}} = M^{FP} + M^{RP} + Nxw \tag{4}$$

where M^{FP} = bending moment developed on the front pile; M^{RP} = bending moment developed on the rear pile; and N = axial force developed on each pile. The last term in Eq. (4) represents the portion of the total moment undertaken through the development of axial forces on the two frame columns (i.e., the piles) via frame action. This reveals that the total moment is undertaken not only through bending deformation of the two piles, but also through axial loading, leading to a substantial decrease of pile distress: the piles are more effective when subjected to axial loading.

This conclusion is of the utmost importance when it comes to the design of piles in which the actual value of the ultimate RF is indeed limited by their structural capacity. Therefore, removing part of the bending distress from the column (i.e., the pile), may considerably raise the practically acceptable ultimate RF. In addition, the deformation required to mobilize the axial resistance of the piles is substantially lower than that required to mobilize the lateral resistance. Therefore, the moment provided by the framing action can be mobilized at relatively small deformations, which is an additional benefit considering the serviceability of the slope being stabilized.

However, this improvement is the result of the distribution of the total system moment to a larger number of piles connected through a pile cap, which means that it is associated with a cost increase. Therefore, it is necessary to parametrically investigate the effectiveness of such alternative configurations, with due consideration to both the expected performance and the corresponding cost.

Definition of Equivalent Pile Frames and Parametric Analysis Setup

As shown in Fig. 13, the equivalent pile frame configuration refers to a pile group consisting of the same number of piles as the single pile configuration (per unit width). Therefore, if single piles are spaced at distance S [Fig. 13(a)], then the equivalent pile frames (each consisting of two pile rows) are spaced at $2S$ [Fig. 13(b)], for the total number of piles (per unit width) to remain the same.

As previously discussed, despite the improvement in terms of the development of bending moment and pile displacement, there still remains doubt as to the optimum effectiveness of pile-frame

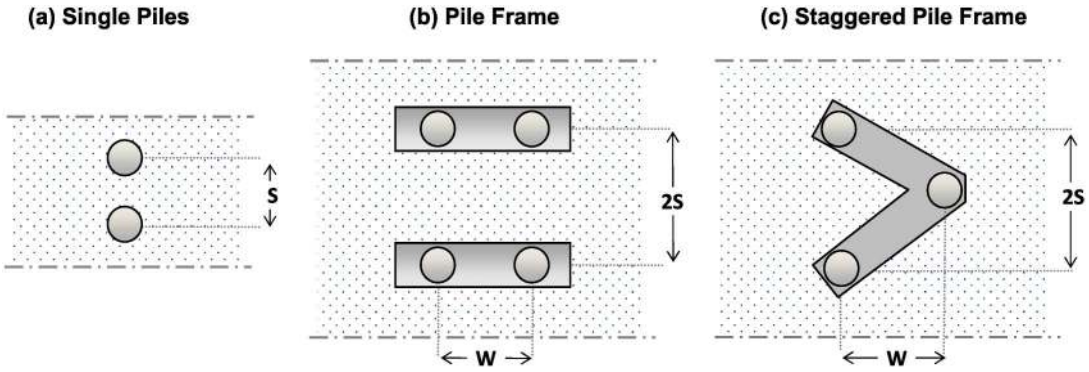

Fig. 13. Definition of the equivalent pile-frame configuration: (a) single piles; (b) two-pile frame; (c) staggered pile frame

systems because the shadow effect remains an unresolved issue, in the sense that trailing piles are under-exploited. A pile lying directly behind another pile will not contribute as substantially to the increase of the total RF. This is defined as shadow effect, which is created from the front pile to the rear pile (Reese et al. 1992; Poulos and Davis 1980), causing the action of soil against the rear pile to be more minimal than that against the front pile. Analytical results (e.g., Poulos and Davis 1980) reveal that the rear pile may develop approximately 20% of the front pile's resistance, depending on distance. The shadow effect diminishes as the distance between the piles increases.

To overcome this inherent disadvantage of pile frames (while maintaining the frame action guaranteed by the pile cap), an alternative pile arrangement has also been considered : a staggered pile frame, schematically illustrated in Fig. 13(c). In this case, the rear (trailing) pile is not positioned directly behind the front piles, but at middistance between the two front piles. In addition to diminishing the shadow effect, this configuration can be more economical because the total length of the pile cap is reduced. Moreover, the multiple soil arching effects that can develop for this arrangement provide increased resistance to soil movements (Chen and Martin 2002; Chen and Poulos 1993; Bransby and Springman 1999).

To unravel the effectiveness of the aforementioned pile group configurations, a numerical parametric analysis is conducted. The simple frames are spaced at $S = 4D$, which is equivalent to single piles spaced at $S = 2D$. No alternative spacing has been examined for the simple frame configuration, because a denser spacing would not be economical and a larger spacing would not provide the necessary arching effect. For the staggered pile group, the spacing is varied at $S = 2D$, $3D$, and $4D$ (referring to the horizontal, i.e., perpendicular to the slope, distance between the front and the rear pile).

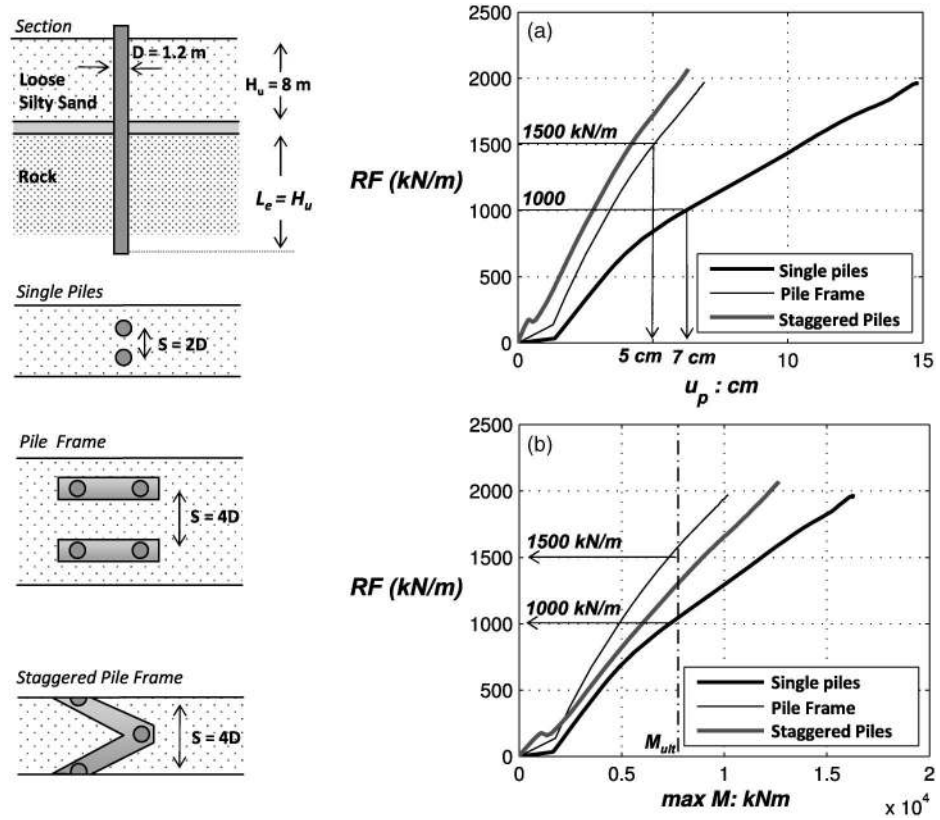

Fig. 14. Comparison of single piles with equivalent pile frames; RF per unit width with respect to (a) pile head displacement u_p; (b) maximum bending moment M

Effectiveness of Pile Group Configurations

Fig. 14 presents a comparison for $D = 1.2$ m and $L_e = H_u$ reinforced concrete piles with equivalent simple and staggered pile frames, for $H_u = 8$ m unstable ground layer of loose silty sand overlying a stiff stable ground (rock). To focus on the comparison in terms of pile group configuration, the effect of embedment depth is not examined at this stage. The case examined here refers to equivalent single pile spacing $S/D = 2$.

Quite interestingly, the ultimate value of lateral RF is the same for all three configurations [Fig. 14(a)]. However, if we consider the noninfinite structural capacity of the piles, this conclusion is modified. For a heavily reinforced concrete pile of $M_{ult} \approx 7.2$ MNm, the maximum realistic RF per unit width that may be offered by the single pile is $RF^{SP} = 1000$ kN/m at 7 cm head displacement [Fig. 14(b)]. For the same structural capacity, the simple frame pile-group can sustain $RF^{GP} \approx 1400$ kN/m at less than 5 cm head

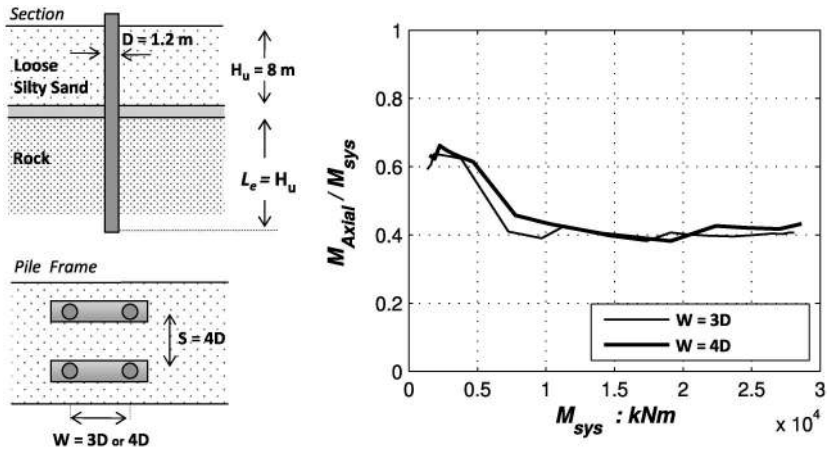

Fig. 15. The effect of the frame arm w: ratio of system moment assumed through pile axial forces M_{axial} to the total moment developed by the system M_{sys} with respect to M_{sys}

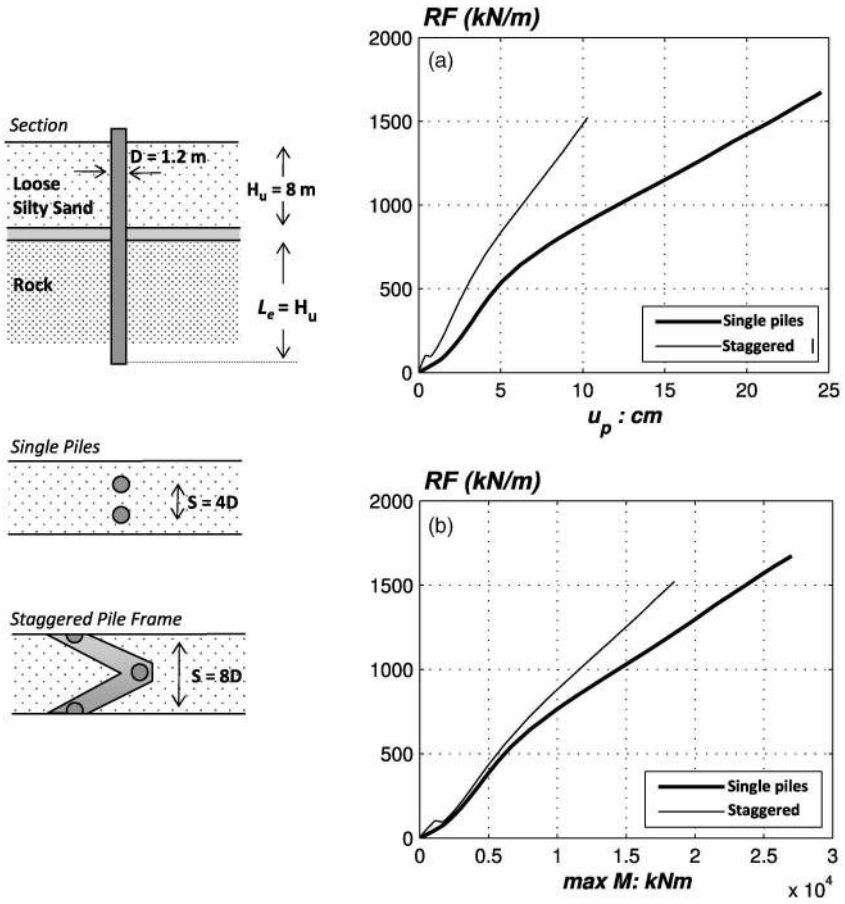

Fig. 16. Comparison of simple with equivalent staggered pile group; RF per unit width with respect to (a) pile head displacement u_p; (b) maximum pile bending moment M

displacement. This corresponds to a 40% increase of RF for the same number of piles per unit width, which is achieved at pile head displacement reduced by 30%. The staggered pile group is less efficient, but still performs better than the single pile configuration.

The effect of the length of the frame arm w is investigated to unravel its effect on the proportion of system moment undertaken by axial forces. Fig. 15 compares the response of the same pile-group (discussed previously) for two different values of frame arm ($w = 3D$ and $4D$) in terms of the ratio M_{axial}/M_{sys} with respect to M_{sys}, where M_{axial} is the amount of moment assumed through pile axial forces (frame effect); and M_{sys} is the total moment developed by the system.

In both cases, the proportion of moment assumed by axial forces is approximately 40% of the total moment. This corresponds to a very effective frame action in both cases, because only approximately half of the total moment is resisted by pile bending. Although an increased arm length may result in enhanced frame effect, the analyses do not show a significant difference between the two cases.

Fig. 16 compares the behavior of single piles spaced at $S = 4D$ with the equivalent staggered pile group configuration for the same soil profile and interface location. An equivalent simple frame configuration is not considered because this would require a frame spacing of $8D$, which does not provide sufficient arching. The two systems exhibit similar behavior. For a structural capacity of $M_{ult} = 7.2$ MNm, the maximum RF per unit width that may be offered by the single piles is $RF^{SP} = 650$ kN/m at 7 cm head displacement, and for the staggered pile group arrangement, this figure increases to $RF^{Stag} = 750$ kN/m at 4 cm head displacement. This corresponds to a small but not unimportant increase in RF of approximately 15%, utilizing the same numbers of piles per unit width, and at the same time pile deflection is decreased by 40%.

Conclusions

This paper has examined a hybrid methodology for the design of slope stabilizing piles [presented and thoroughly validated in Kourkoulis et al. (2009)] to derive insights into the factors affecting the response, and to produce dimensionless design charts useful in practice. The key conclusions are as follows:

1. A pile spacing $S \leq 4D$ is required to generate soil arching between the piles. For $S > 5D$, the piles will behave as single piles, and the soil may flow between them. Hence, such an arrangement cannot be applied for slope stabilization. $S = 4D$ is considered to provide the most cost-effective solution: it has the largest spacing (i.e., with the least amount of piles) required to produce soil arching between the piles, so that the inter-pile soil will be adequately retained. This conclusion is in accord with practice, where spacings between $3D$ and $5D$ are typically implemented.
2. For the cases examined, soil inhomogeneity in terms of shear modulus was found to be unimportant. The response is primarily affected by the strength of the unstable soil and not by the distribution of stiffness.
3. When the piles are embedded in a substratum of relatively low strength, a large pile deflection is required to reach the same level of ultimate RF as when embedded in a stiff substratum.
4. For a small pile embedment, the response of the pile is dominated by rigid-body rotation without substantial flexural distortion. This finding is consistent with Poulos's (1999) description of the short pile mode of failure, which involves mobilization of the stable soil strength and failure of the soil underneath the pile. Therefore, the pile structural capacity is not adequately exploited, and the design will not be economical. However, if the stable stratum is of high strength, the increase of embedment length will unavoidably be associated with an increased installation cost. Such cost implications have not been examined in this paper.
5. The critical embedment depth L_e to achieve fixity conditions at the base of the pile depends on the relative strength of the stable ground $(P_u)_{stable}$ compared to that of the unstable ground $(P_u)_{unstable}$. It is found to range from $1.5H_u$ for $(P_u)_{stable} = (P_u)_{unstable}$ to $0.7H_u$ for $(P_u)_{stable} = 3(P_u)_{unstable}$, where H_u is the thickness of the unstable soil.
6. An attempt was made to produce dimensionless design charts useful in practice. The example presented refers to reinforced concrete piles embedded in hard rock. The embedment length L_e was assumed equal to the unstable soil layer depth H_u, which was found adequate to provide fixity conditions. Results were presented for two characteristic slenderness ratios and pile spacing in terms of dimensionless pile resistance force with respect to dimensionless pile displacement.
7. Single piles (especially if not combined with tiebacks) may be inadequate for stabilization of deep landslides. In such cases, pile-groups may be the most efficient solution. With single piles, the system moment can only be undertaken through bending of the pile, but in a pile group almost half of the system moment is assumed by axial forces (frame effect). For the same number of piles per unit width, a 40% increase of RF can be achieved through use of a pile group.

Acknowledgments

This work was partially supported by the EU 7th Framework research project funded through the European Research Council's (ERC) "Ideas" Programme, in support of Frontier Research—Advanced Grant Contract No. ERC-2008-AdG 228254-DARE.

References

Barenblatt, G. I. (1996). *Scaling, self-similarity, and intermediate asymptotics*, Cambridge University Press, Cambridge, UK.

Bishop, A. W. (1955). "The use of the slip circle in the stability analysis of slopes." *Geotechnique*, 5(1), 7–17.

Bransby, M. F., and Springman, S. M. (1999). "Selection of load-transfer functions for passive lateral loading of pile groups." *Comput. Geotech.*, 24(3), 155–184.

Broms, B. (1964). "Lateral resistance of piles in cohesionless soils." *J. Soil Mech. and Found. Div.*, 90, 123–156.

Chen, C., and Martin, G. (2002). "Soil-structure interaction for landslide stabilizing piles." *Comput. Geotech.*, 29(5), 363–386.

Chen, L. T., and Poulos, H. G. (1993). "Analysis of pile-soil interaction under lateral loading using infinite and finite elements." *Comput. Geotech.*, 15(4), 189–220.

Cox, W. R., Dixon, D. A., and Murphy, B. S. (1984). "Lateral load tests of 5.4 mm piles in very soft clay in side-side and in-line groups." *Laterally loaded deep foundations: Analysis and performance*, ASTM, West Conshohocken, PA.

D'Appolonia, E., Alperstein, R., and D'Appolonia, D. J. (1967). "Behaviour of colluvial slope." *J. Soil Mech. and Found. Div.*, 93, 447–473.

De Beer, E. E., and Wallays, M. (1972). "Forces induced in piles by unsymmetrical surcharges on the soil round the piles." *Proc., 5th Conf. on Soil Mechanics and Foundation Engineering*, Vol. 1, Spanish Society for Soil Mechanics and Foundation, Madrid, Spain, 325–32.

Gazetas, G., and Dobry, R. (1984). "Horizontal response of piles in layered soils." *J. Geotech. Eng.*, 110(1), 20–40.

Heyman, L., and Boersma, L. (1961). "Bending moment in piles due to lateral earth pressure." *Proc., 5th ICSMFE*, Vol. 2, 425–429.

Hull, T. S. (1993). "Analysis of the stability of slopes with piles." *11th Southeast Asian Geotechnical Conf.*, Southeast Asian Geotechnical Society, Singapore, 639–643.
Ito, T., and Matsui, T. (1975). "Methods to estimate lateral force acting on stabilizing piles." *Soils Found.*, 15(4), 43–60.
Janbu, N. (1957). "Earth pressures and bearing capacity calculations by generalised procedure of slices." *Proc. 4th Int. Conf. Soil Mech. Found. Eng.*, Vol. 2, 207–212.
Kitazima, S., and Kishi, S. (1967). "An effect of embedded pipes to increase resistance against circular slides in soft clay foundation." *Technical Note of Port and Harbour Research Institute*, Vol. 29, 63–94 (in Japanese).
Kourkoulis, R. (2009). "Interplay of mat foundations and piles with a failing slope." Ph.D. thesis, National Technical Univ. of Athens, Greece.
Kourkoulis, R., Gelagoti, F., Anastasopoulos, I., and Gazetas, G. (2010). "Hybrid method for analysis and design of slope stabilizing piles." *J. Geotech. Geoenviron. Eng.*, in press.
Langhaar, H. L. (1951). *Dimensional analysis and theory of models*, Wiley, New York.
Leussink, H., and Wenz, K. P. (1969). "Storage yard foundations on soft cohesive soils." *Proc., 7th ICSMEE*, Vol. 2, 149–155.
Liang, R. and Zeng, S. (2002). "Numerical study of soil arching mechanism in drilled shafts for slope stabilization." *Soils and foundations*, Vol. 42 (2), Japanese Geotechnical Society, 83–92.
Matlock, H. (1970). "Correlations for design of laterally loaded piles in soft clay." *Proc., 2nd Annual Offshore Technology Conf.*, 577–594.
Nicu, N. D., Antes, D. R., and Kesslerr, S. (1971). "Field measurements on instrumented piles under an overpass abutment." *Highway Research Record 354*, Highway Research Board, Washington, DC.
Oakland, M. W., and Chameau, J. L. A. (1984). "Finite-element analysis of drilled piers used for slope stabilization." *Laterally loaded deep foundations: Analysis and performance*, ASTM, West Conshohocken, PA, 182–93.
Palmer, A. C. (2008). *Dimensionless analysis and intelligent experimentation*, World Scientific, Singapore.
Poulos, H. G. (1995). "Design of reinforcing piles to increase slope stability." *Can. Geotech. J.*, 32(5), 808–818.
Poulos, H. G. (1999). "Design of slope stabilizing piles." *Slope stability engineering*, J. C. Jiang, N. Yagi, and T. Yamagami, eds., Balkema, Rotterdam, Netherlands.
Poulos, H. G., and Chen, L. T. (1997). "Pile response due to excavation-induced lateral soil movement." *J. Geotech. Geoenviron. Eng.*, 123(2), 94–99.
Poulos, H. G., and Davis, E. H. (1980). *Pile foundation analysis and design*, Wiley, New York.
Poulos, H. G., and Hull, T. S. (1989). "The role of analytical geomechanics in foundation engineering." *Foundation engineering: Current principles and practice*, Vol. 1, F. H. Kulhawy, ed., ASCE, New York, 485–499.
Pradel, D., and Carrillo, R. (2008). "Landslide stabilization using drilled shafts." *Continuum and distinct element numerical modeling in geo-engineering (Proc., 1st Int. FLAC/DEM Symp.)*, R. Hart, C. Detournay, and P. Cundall, eds., Itasca Consulting Group, Minneapolis.
Prakash, S. (1962). "Behavior of pile groups subjected to lateral load." Ph.D. dissertation, Dept. of Civil Engineering, Univ. of Illinois.
Randolph, M. F. (1981). "The response of flexible piles to lateral loading." *Geotechnique*, 31(2), 247–259.
Randolph, M. F., and Houlsby, G. T. (1984). "The limiting pressure on a circular pile loaded laterally in cohesive soil." *Geotechnique*, 34(4), 613–623.
Reese, L. C., and Van Impe, W. F. (2001). *Single piles and pile groups under lateral loading*, Balkema, Rotterdam, Netherlands.
Reese, L. C., Wang, S. T., and Fouse, J. L. (1992). "Use of drilled shafts in stabilizing a slope." *Stability and performance of slopes and embankments*, Vol. 2, ASCE, Reston, VA, 1318–1332.
Sarma, S. K. (1973). "Stability analysis of embankments and slopes." *Geotechnique*, 23(3), 423–433.
Smethurst, J. A., and Powrie, W. (2007). "Monitoring and analysis of the bending behaviour of discrete piles used to stabilise a railway embankment." *Géotechnique*, 57(8), 663–677.
Spencer, E. (1967). "A method of analysis of the stability of embankments assuming parallel interslice forces." *Geotechnique*, 17(1), 11–26.
Viggiani, C. (1981). "Ultimate lateral load on piles used to stabilize landslides." *Proc., 10th. Int. Conf. Soil Mechanics and Foundation Engineering*, Vol. 3, Balkema, Rotterdam, Netherlands, 555–560.
Wang, W. L., and Yen, B. C. (1974). "Soil arching in slopes." *J. Geotech. Eng. Div.*, 100(1), 61–78.
XTRACT, Ver. 3.0.3 [Computer software]. Imbsen and Associates, Sacramento, CA.